PNAS
www.pnas.org

Supplementary Information for

Rerouting of ribosomal proteins into splicing in plant organelles

Chuande Wang[1], Rachel Fourdin[1], Martine Quadrado[1], Céline Dargel-Graffin[1], Dimitri Tolleter[2], David Macherel[2] and Hakim Mireau[1*]

[1] Institut Jean-Pierre Bourgin, INRAE, AgroParisTech, Université Paris-Saclay, 78000, Versailles, France
[2] Université d'Angers, Unité Mixte de Recherche 1345, Institut de Recherche en Horticulture et Semences, Angers 49045, France

*To whom correspondence should be addressed. Email: hakim.mireau@inra.fr

This PDF file includes:

www.pnas.org/cgi/doi/10.1073/pnas.2004075117

Supplementary Information

SI Materials and Methods

Plant material

Arabidopsis (*Arabidopsis thaliana*) Col-0 plants were obtained from the Arabidopsis stock centre of the Institut National de Recherche pour l'Agriculture, l'Alimentation et l'Environnement in Versailles (http://dbsgap.versailles.inra.fr/portail/). The Arabidopsis *ul18-l1* (N581267) and *ul18-l8* (N568525 and CS841212) mutants were obtained from the SALK mutant collection (1). Plants were grown in a greenhouse in long day conditions for 10 to 12 weeks before use. Flowers or leaves were harvested simultaneously for all genotypes, snap-frozen in liquid nitrogen and stored at -80°C until use.

For the complementation assays, the coding sequence of *uL18-L1* or *uL18-L8* without stop codon but with 1 kb of promoter region was amplified by PCR and cloned to pGWB13 (2) by Gateway™ cloning, creating C-terminal translational fusions with the 3HA tag. The resulting plasmids were used to transform *ul18-l1* or *ul18-l*8-1 heterozygous plants by floral dipping and complemented homozygous mutant plants were identified in the progenies of transgenic plants.

Preparation of organelles and stromal protein

Arabidopsis mitochondria and chloroplasts were purified from flower buds and young leaves, respectively, as described in (3). Stromal protein fractions were prepared from purified plastids as previously described in (4).

Immunodetection of proteins

Proteins were extracted from flowers, leaves or purified organelles in 30 mM HEPES-KOH (pH 7.7), 10 mM $Mg(OAc)_2$, 150 mM KOAc, 10% glycerol and 0.5% (w/v) CHAPS. Protein concentrations were measured using Bradford reagents (Bio-Rad) and separated by SDS-PAGE. After electrophoresis, gels were transferred onto PVDF membranes (Bio-Rad) under semidry conditions. Membranes were hybridized with antibodies using dilutions indicated in Table S2.

Subcellular distributions of uL18-L1 and uL18-L8 proteins

DNA regions corresponding to the coding sequence of each uL18-Like protein but lacking the stop codon were PCR amplified and transferred into pGWB5 (2) by Gateway™ cloning (Invitrogen) to create GFP translational fusions. The constructs were used to transform Arabidopsis plants by floral dipping and GFP fluorescence was visualized in leaf or root cells by confocal microscopy. When necessary, roots of transgenic plants were soaked in a solution of 0.1 µM MitoTracker™ Red to label mitochondria prior to observation.

RNA analysis

RNA extraction, northern blot and quantitative RT-PCR analyses were done as previously described in (5) with primer sets detailed in (6, 7).

RNA immunoprecipitation assays

Immunoprecipitation of uL18-L1-3HA and uL18-L8-3HA were performed using the μMACS HA-Tagged Protein Isolation Kit (Miltenyi Biotec). Briefly, total proteins were extracted from 1 g of Arabidopsis transgenic cells expressing either uL18L1-3HA or uL18L8-3HA in 1 mL of cold lysis buffer (20 mM HEPES-KOH, pH 7.6, 100 mM KCl, 20 mM $MgCl_2$, 1 mM DTT, 1% Triton X-100, 1X of complete EDTA-free protease inhibitor (Roche)) for 30 mins on ice. The lysates were clarified by centrifugation at 100,000 *g* for 20 mins at 4°C and resulting supernatants were incubated with 50 μL of anti-HA magnetic beads or protein A magnetic beads (Thermo Fisher Scientific) for 1 h at 4°C with rotation (10 rpm). After three washes with 1 mL of washing buffer (lysis buffer with only 0.1% Triton X-100), proteins were eluted in 120 μL of elution buffer provided by the kit and then subjected to immunoblot analysis. Co-immunoprecipitated RNAs were extracted with TRI Reagent® (Invitrogen) and treated with the RTS DNase I (Mobio) prior to RT-qPCR analysis. RNAs representing 1% of the input fraction and the totality of immunoprecipitated RNAs were used for cDNA synthesis. Three microliters of 10-fold diluted cDNA solutions were used in each qPCR reaction.

Blue Native gel and in-gel activity assays

One hundred micrograms of mitochondrial proteins were separated on 4-16% (w/v) polyacrylamide Native PAGE gels (Invitrogen) and then either transferred to PVDF membranes or subjected to in-gel activity staining as in previously described in (5). After electrophoresis, the separated protein complexes were transferred to PVDF membranes for immunoblotting or stained in Coomassie blue R-250. Antibodies listed in Table S2 were used for immuno-detection.

Sucrose density gradient centrifugation

One gram of transformed Arabidopsis cells and the equivalent of 3 to 6 mg of stromal or total mitochondrial proteins were resuspended in 1 mL (for cells) or 200 μL (for organelles) of lysis buffer (30 mM HEPES-KOH (pH 7.8), 100 mM KOAc, 10 mM $Mg(OAc)_2$, 5 mM β-mercaptoethanol, 5% glycerol, 1% n-dodecyl β-D-maltoside [DDM] and 1X cOmplete™ EDTA-free protease inhibitor (Roche)) and incubated at 4°C for 30 mins. The lysates were then diluted with the same volume of lysis buffer with no DDM and then cleared by ultracentrifugation at 100,000 *g* for 20 mins. Volumes corresponding to 2 mg of proteins were layered on continuous sucrose gradients (10%-30%) made in lysis buffer without DDM. Sucrose gradients were ultracentrifuged at 268,000 *g* for 4 hours at

4°C. Gradients were fractionated into 16 fractions of 330 µL and subsequently analysed by immunoblotting.

Transformation of Arabidopsis cell suspension cultures

The coding sequences of *uL18-L1* and *uL18-L8* without their stop codon were PCR amplified and transferred by Gateway™ cloning (Invitrogen) into pGWB14 (2) resulting in C-terminal fusions with the 3xHA coding sequence, expressed under the control of the 35S promoter. These constructs were used to transform an Arabidopsis cell culture as indicated in (8).

Analysis of photosynthesis and pigment composition

Plants were grown in long-day conditions (16:8 hours, 19:21°C L:D) at 120 µmol photons.m^{-2}.s^{-1} for 4 weeks. Water content of rosette leaves was estimated by measuring the fresh and dry weight (after 48 h at 90°C) of detached rosettes. Leaf chlorophyll and carotenoid pigments were extracted with dimethylformamide and measured according to (9). Chlorophyll fluorescence of rosettes was measured non-invasively at room temperature with a PSI Open FluorCam FC 800-O (Photon Systems Intruments). For each plant, 13 spots, one per leaf (9 spots of 0.02 mm^2 about 500 pixels and 4 spots of 0.01 mm^2 about 200 pixels) were used to get a spatial average of fluorescence over time. Maximum fluorescence was obtained by saturation pulses at 2,800 µmol photons m^{-2}.s^{-1} for 600 ms. Chlorophyll fluorescence parameters (F_v/F_m, 1-qP, qL, NPQmax, NPQrelax) were calculated from $F_{m'}$ (F_m if after 45 mins of dark adaption), F_0' (F_0 if after 45 mins of dark adaption) and F as maxima, minimal and current fluorescence respectively. Actinic light (420 µmol photons.m^{-2}.s^{-1}) was turned on for 500 s (with a saturating pulses every 80 s) and then dark relaxation time for 280 s (with saturating pulse at 80 s and then 200 s later). The maximum quantum efficiency of PSII photochemistry, Fv/Fm, was calculated as (Fm-Fo)/Fm, the Photochemical quenching, 1-qP as 1-($F_{m'}$-F)/($F_{m'}$-$F_{0'}$), the fraction of open PSII centres, qL as ($F_{m'}$-F)/($F_{m'}$-$F_{0'}$), and the Non Photochemical Quenching, NPQ as (F_m-$F_{m'}$)/$F_{m'}$ with NPQ_{max} just before turning the light off and NPQ_{relax} at the end of the 280 s of relaxation period of dark.

Supplemental Figures

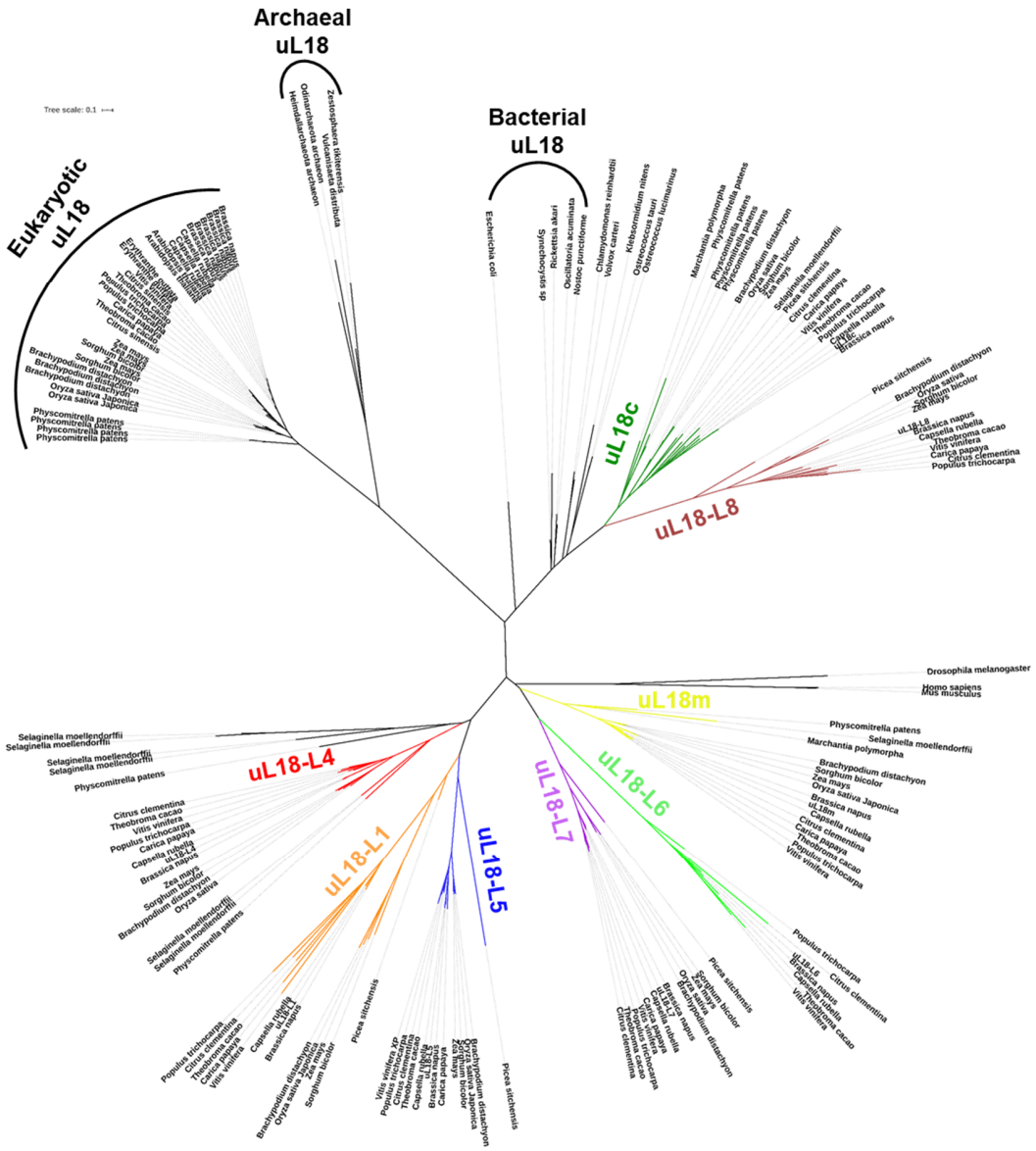

Fig. S1. The uL18 and uL18-like proteins are conserved in monocots and dicots. Sequence distance neighbor-joining tree of uL18 or uL18-like protein homologs from a selected panel of bacteria, archebacteria, animalia, chlorophyta, bryophytes, gymnosperms, dicotyledons and monocotyledons. All accession numbers of the proteins reported here are listed in Table S3. These alignments reveal likely orthologs for each Arabidopsis uL18-like in monocots and dicots, supporting their functional conservation in terrestrial plants. The tree was generated using MEGA7 (www.megasoftware.net) and visualized with iTOL (Interactive Tree Of Life, https://itol.embl.de/).

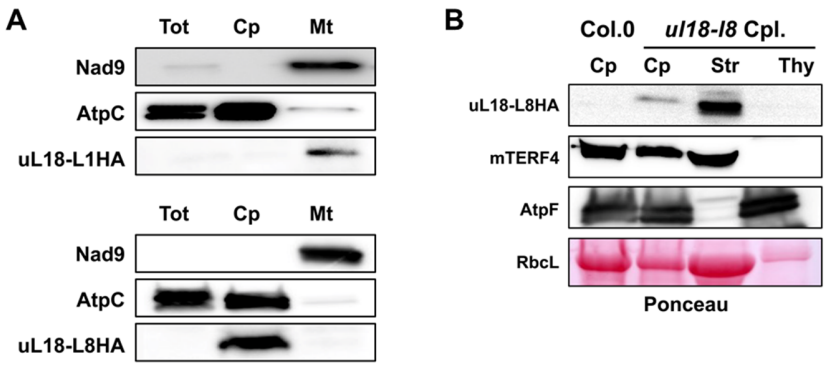

Fig. S2. Subcellular distributions of uL18-L1 and uL18-L8 proteins. (A) Total (Tot), chloroplast (Cp) and mitochondrial (Mt) protein extracts were prepared from genetically complemented *ul18-l1* and *ul18-l8-1* lines and analyzed by immunoblot assays with the indicated antibodies. The detection of the plastid ATP synthase subunit C (AtpC) and the mitochondrial NADH dehydrogenase subunit 9 (Nad9) were used to control the purity of plastid and mitochondrial extracts, respectively. The anti-HA monoclonal antibody was used to detect the uL18-L1-HA and uL18-L8-HA fusion proteins. (B) Detection of the uL18-L8 protein in chloroplast (Cp), stromal (Str) and thylakoid (Thy) fractions by immunoblot analysis. Antibodies to mTERF4 and AtpF were used as control for stromal and thylakoid fractions, respectively. A cropped image of one of the blot stained with Ponceau S illustrates the abundance of the stromal protein RbcL in the different fractions.

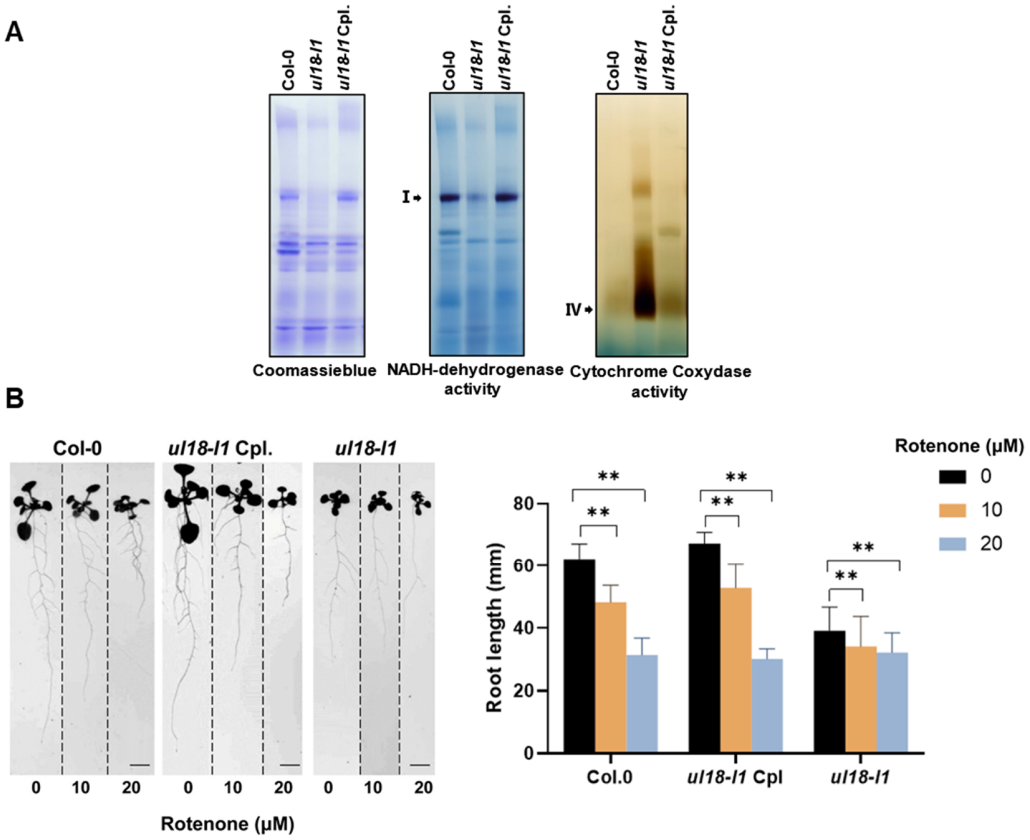

Fig. S3. *ul18-l1* plants are complex I mutants. (A) Mitochondrial protein extracts prepared from wild-type (Col-0), mutant (*ul18-l1*) and complemented (Cpl) plants, separated in BN-PAGE gels and then stained with Coomassie blue or by in gel activity staining to estimate complex I (NADH dehydrogenase) and complex IV (cytochrome *c* oxidase) accumulation levels. (B) Primary root length of wild-type (Col-0), mutant (*ul18-l1*) and complemented plants (Cpl) measured in the absence or in the presence of 10 mM or 20 mM of the complex I inhibitor rotenone. Plants were grown on vertical squared plates for 14 (Col-0 and Cpl) or 24 (*ul18-l1*) days prior to measurements (left panel). The values (right panel) are means of three independent biological replicates (error bars indicate SD). Asterisks indicate statistically significant differences between the inhibitor-treated versus the no-inhibitor conditions, for each genotype (Student's t test for paired samples, P, 0.01).

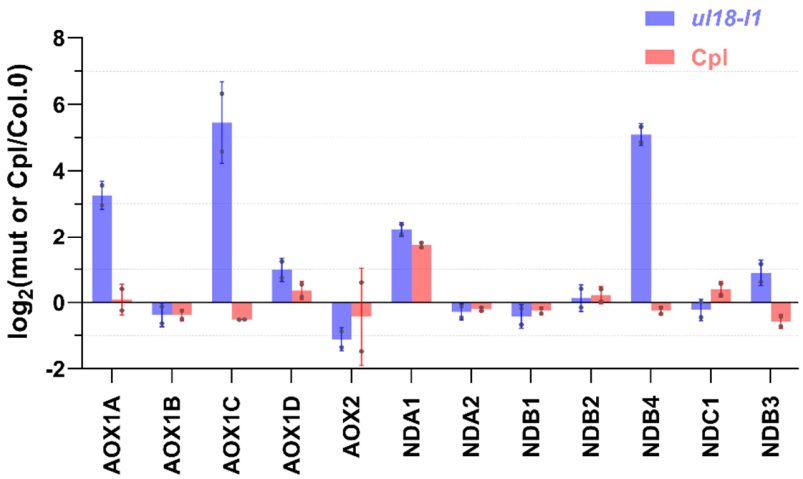

Fig. S4. The alternative respiratory pathway is induced in *ul18-l1* mutant plants. Quantitative RT-PCR results measuring the relative accumulation levels of alternative oxidase (*AOX*) and NADH dehydrogenase (*NDA*, *NDB* and *NDC*) transcripts in *ul18-l1* mutant and complemented (Cpl) plants. Log_2 ratios of mutant (blue bars) or Cpl (red bars) to wild-type are shown. Two biological repeats and three technical repeats were performed for each genotype in this analysis.

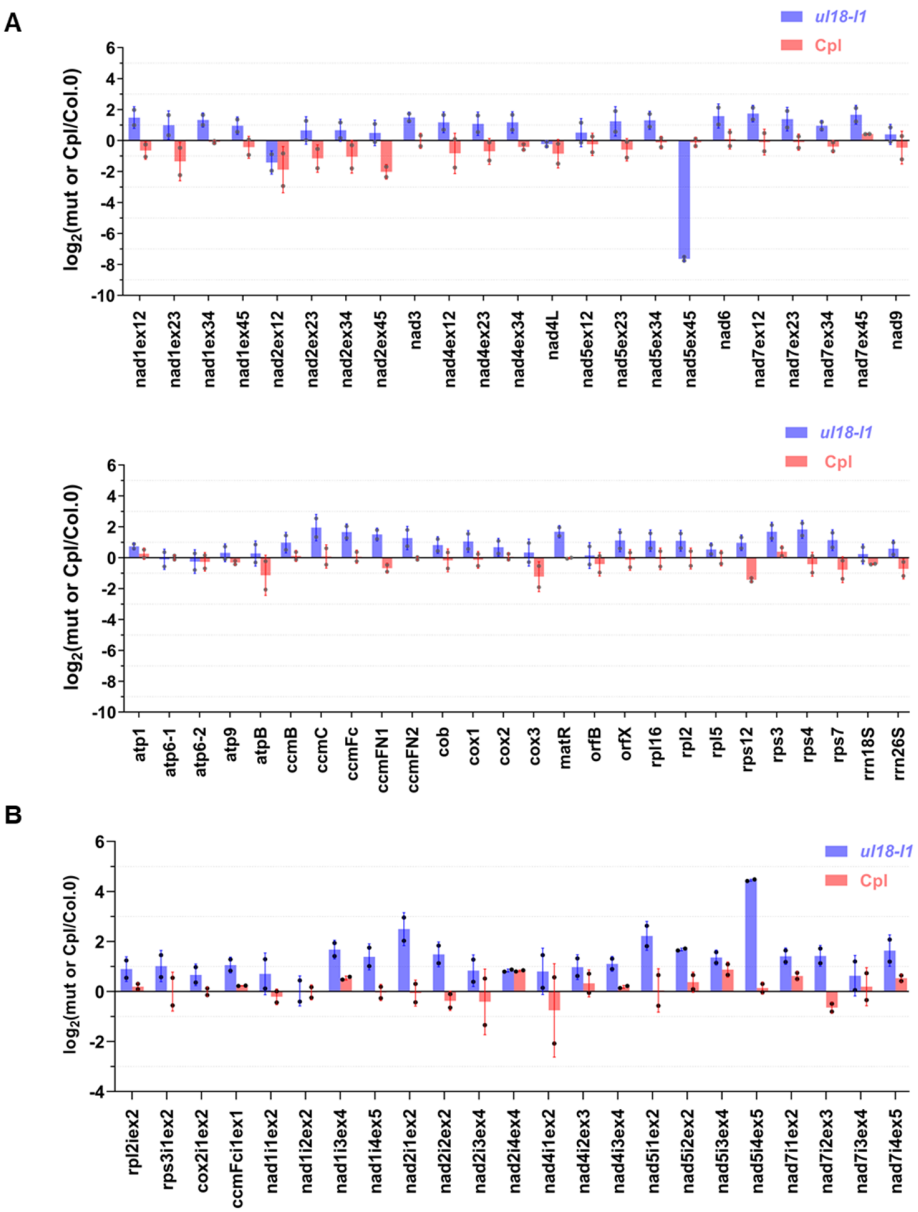

Fig. S5. Quantitative RT-PCR analysis measuring the accumulation levels of precursor and mature mitochondria-encoded mRNAs in *ul18-l1* and complemented (Cpl) plants. (A) For mature mRNA quantification, a single PCR was performed for transcripts containing a sole exon. For intron-containing mRNAs, PCR were done using primer pairs across each intron. (B) Precursor mRNAs were specifically quantified using primers situated across the indicated intron (i) - exon (ex) junctions. The bars show $\log_2$ ratios of mRNA abundance in *ul18-l1* (blue bars) and complemented (red bars) plants to the wild type (Col-0). Three technical replicates and two independent biological repeats were used for each genotype. Standard errors are indicated.

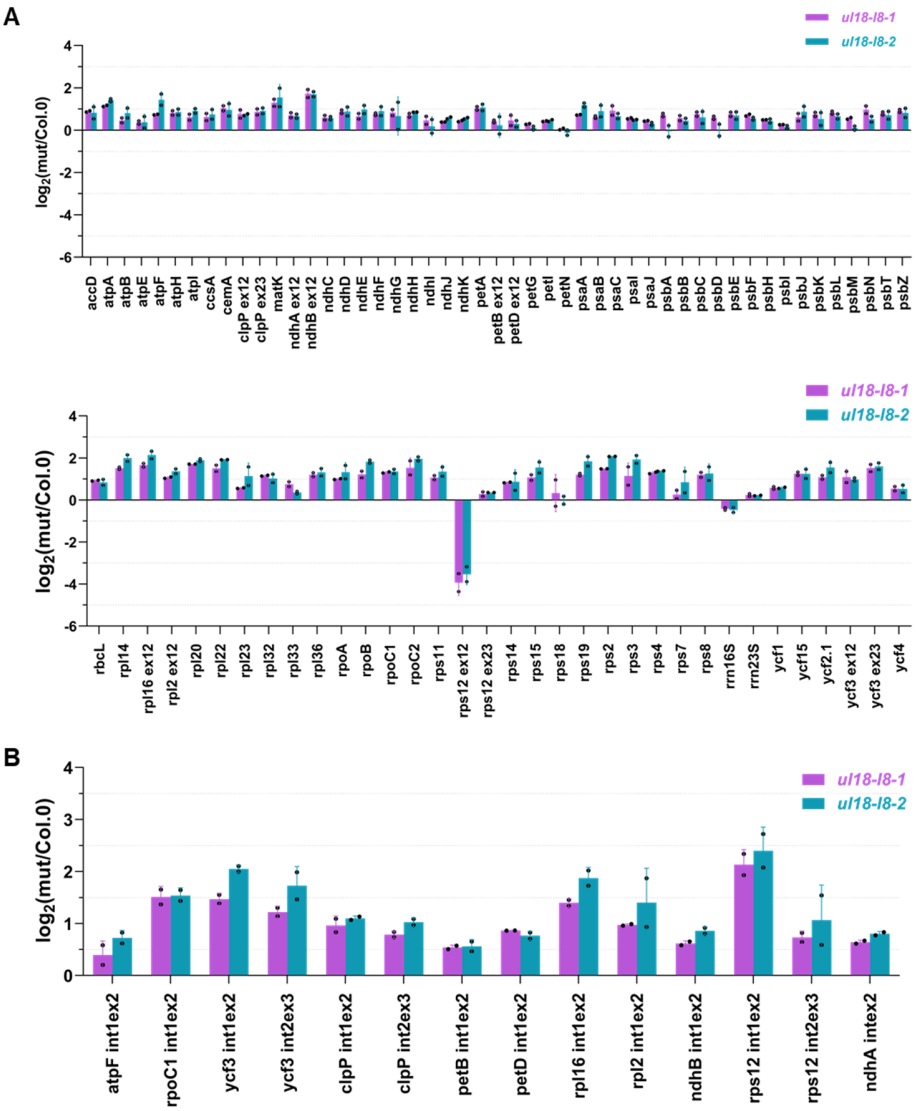

Fig. S6. Quantitative RT-PCR analysis measuring the accumulation levels of precursor and mature plastid-encoded mRNAs in *ul18-l8* mutants. (A) For mature mRNA quantification, a single PCR was performed for transcripts containing a sole exon. For intron-containing mRNAs, PCR were done using primer pairs across each intron. (B) Precursor mRNAs were specifically quantified using primers situated across the indicated intron (i) - exon (ex) junctions. The graphs depict the $\log_2$ ratios of transcript levels in the mutants as compared with those in wild-type. Three technical replicates and two independent biological repeats were used for each genotype. Standard errors are indicated.

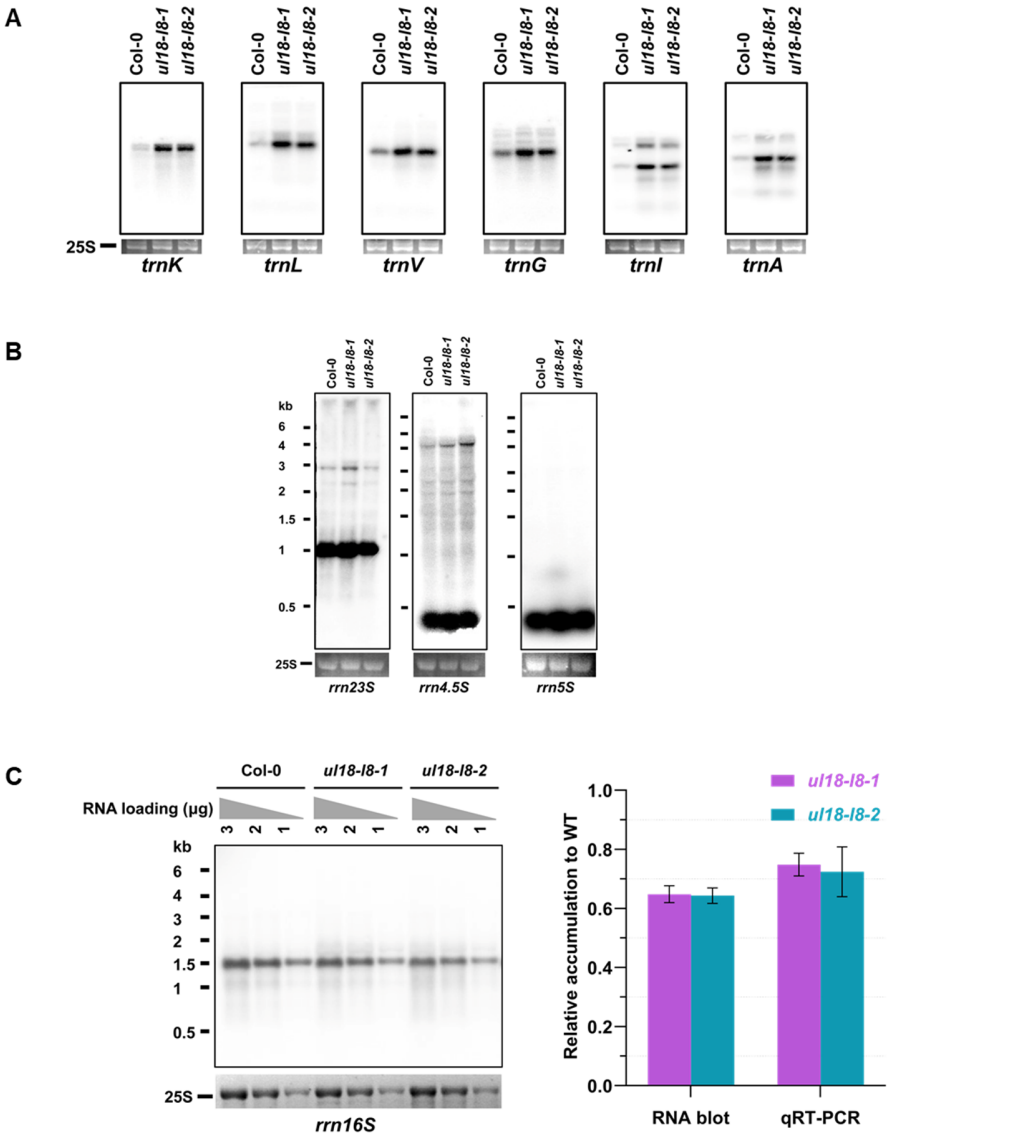

Fig. S7. Plastid tRNAs and rRNA accumulation in *ul18-l8* mutants. The blots were performed on total RNA of the indicated genotypes and used probes are mentioned below each blot. (A) RNA gel blot hybridizations showing the steady state levels of plastid tRNAs. (B) RNA gel blot analyses measuring the steady state levels of the plastid-encoded 23S, 4.5S and 5S rRNAs. Ethidium bromide staining of 25S RNA is shown below the blots and serves as a loading control. (C) RNA gel blot analyses performed on 1, 2 and 3 µg of total RNA and measuring the steady state levels of the plastid-encoded 16S rRNA. The graphs (right) depict average ratios of 16S transcript levels in the two mutants compared with those in wild-type, as measured by RNA blot assay and qRT-PCR.

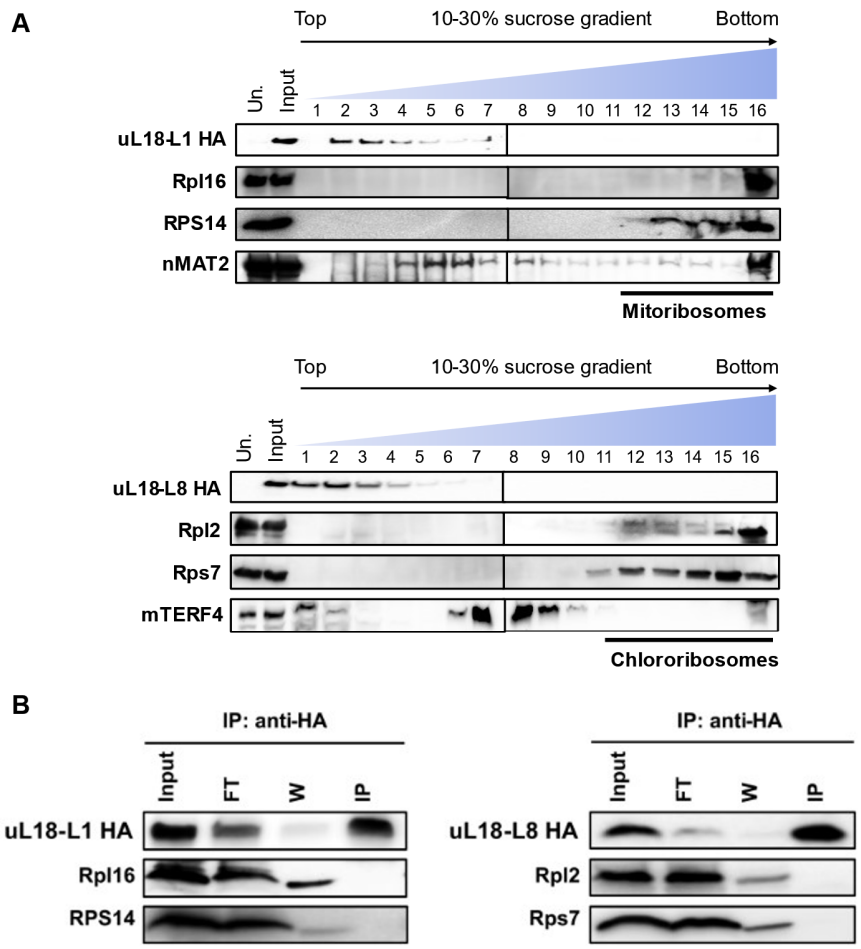

Fig. S8. uL18-L1 and uL18-L8 do not sediment with ribosomes. (A) Arabidopsis extracts prepared from cell lines over-expressing the indicated *uL18-Like* genes were loaded on sucrose gradients. Immunoblots of recovered fractions were probed with antibodies as listed in Figure 7, in addition to nMAT2 which is a nuclear-encoded maturase required for splicing multiple group II mitochondrial introns (10). (B) Immunoprecipitation of uL18-L1-3HA and uL18-L8-3HA. Total extracts from transgenic Arabidopsis cell lines expressing uL18-L1-3HA or uL18-L8-3HA were used for immunoprecipitation with anti-HA antibody. Equal volumes of input, flow-through (FT), wash (W) and immunoprecipitated (IP) fractions were analyzed by immunoblot analysis using the indicated antibodies.

Table S1. A List of Primers Used in This Study.

Primer	Sequence 5'-3'	Experiment
L18L5-7	GCAACGTTTCTTCTCGAACC	Genotyping
L18L5-6	GTGTCTCCGTTTGCCAGATT	
L18-8-1bis	CCGCTGAGGGTAATGTTCTGA	
L18-8-2bis	AGAGTTTGTGGAATGCCCGT	
GWL18L5-8	CAAAAAAGCAGGCTAAAAATTAGAAGACAGTGTGACAAC	Complementation; GFP expression
GWL18L5-7bis	CAAGAAAGCTGGGTCGGCCATCATTAGATGACTAGTCTTC	
GWL18L5-1	CAAAAAAGCAGGCTCTATGGCTTTGATGGTTTTGAG	
GWL18-8B	CAAGAAAGCTGGGTCAGTTTTCGGACTCTCCACTCG	
GWL18-8R	CAAGAAAGCTGGGTCCGGTAAGAACCCGTGTTGCG	
GWL18-8-F	CAAAAAAGCAGGCTAAAATGGCTGCTTTGACTTCTCT	
nad2e1	GCAGAATTCGTTCGGATC	mRNA probes for RNA gel blot
nad2e8	TATGAACTGAGTGCCATTTGA	
nad5 E7	AGAAGGAAGCGCTATAATGAC	
nad5 E6	TACTCACTATCAAAATGAAAG	
nad5 intron3b-1	GAGTCGATACCTTGCTCGCC	
nad5 intron3b-2	CGCCTATTACACGGCTCACT	
nad5 intron4-1	TCCCTATGGACAAGGGGACA	
nad5 intron4-2	ACTCTTCATTCTCCCGTGCT	
nad5 exon4-1	TTCAGGTGCTTTTGTTGCGT	
nad5 exon4-2	GGCCAATCGTCGGAATGTGT	
RPS12CpE1-1	AGACAGCCAATCCGAAACGTC	
RPS12CpE1-2	CGAGTACATGTTCCTCGTCG	
RPS12CpI1-1	CATTGGTGCAAATCCAATCAACTC	
RPS12CpI1-2	CACATTCTTTGGCTCTACCCC	
RPS12CpI1-3	TCGAAGAATGAGGGGCAAAGA	
RPS12CpI1-4	TCGCGAATCTCCTCCCTTCT	
RPS12CpE2-1	CCAGAGTACGATTAACCTCGGG	
RPS12CpE2-2	ACTCCGACAGCATCTAGGGT	
RPL20-1	TAGCTCGGAGGCGTAGAACA	
RPL20-2	TTGTGCAAGTATTTTCCGATTAAGA	
RPS7-1	ATGTCACGCCGAGGTACTG	
RPS7-2	GCAAGTGCTTTTCCTTGCGT	
trnA-F	TGGAGATAAGCGGACTCGAACCGC	tRNA probes for RNA gel blot
trnA-R	GGGGATATAGCTCAGTTGGTAGAGCTCCG	
trnV-F	TAGGGCTATACGGACTCGAAC	
trnV-R	AGGGCTATAGCTCAGTTAGGT	
trnK-F	TGGGTTGCCCGGGACTCGAA	
trnK-R	GGGTTGCTAACTCAACGGTAGA	
trnG-F	GCGGGTATAGTTTAGTGGTAAA	
trnG-R	GGGTAGCGGGAATCGAACCC	
trnL-F	GGGGATATGGCGGAATTGGTAG	
trnL-R	TGGGGATAGAGGGACTTGAACC	
trnI-F	GGGCTATTAGCTCAGTGGTAG	
trnI-R	TGGGCCATCCTGGATTTGAAC	

rrn16cp1	TGATTGGGCGTAAAGCGTCT	rRNA probes for RNA gel blot
rrn16cp2	CTTGGTAGTTTCCACCGCCT	
rrn23cp1	AGGCCTCCCAAAAGGTAACG	
rrn23cp2	GTCAAGCTCCCTTCTGCCTT	
rrn5cp1	CCATCCCGAACTTGGTGGTT	
rrn5cp2	GGCGTCGAGCTATTTTTCCG	
rrn4.5cp1	GCGAGACGAGCCGTTTATCA	
rrn4.5cp2	TGCCTCAGCTGCATACATCA	
NAD1exon2_R	GACCAATAGATACTTCATAAGAGACCA	RIP-qPCR for uL18-L1
Qmnad1intron1R	CGTGCTCGTACGGTTCATAG	
QM0285R	GCGAGCAGAAGCAAGGTTAT	
mito091R	CCCATTCCTAACCAGTGGAG	
mito337F	CTTATTCGTGGCAACCTTCC	
QM1320F	TATTTGTTCTTCGCCGCTTT	
QMnad5exon2F	TGGACCAAGCTACTTATGGATG	
QMnad5intron1R	TTCGCAAATAGGTCCGACT	
QMnad5intron2F	GTACGATCGTGTCGGGTGA	
QMnad5exon2R	CTGGCTCTCGGGAGTCTCTT	
QM0060F	AACATTGCAAAGGCATAATGA	
QMnad5intron4R	CCTGTAAACCCCCATGATGT	
QMnad7intron1F	ACGGTTTTTAGGGGGATCTG	
nad7exon2R	AAGGTAAAGCTTGAAGATAAGTTTTGT	
QMccb452intronF	CCCGGATCGAATCAGAGTT	
QM180F	CACATGGAGGAGTGTGCATC	
QM0160R	TGGGGGATTAATTGATTGGA	
mito037R	AGCAGTACGAGCTGAAAGGC	
rps12F	TCTCACACCGGGTAAATCCT	RIP-qPCR for uL18-L8
rps12R	ATCCGAAACGTCACGAAATC	
rps12_exon3F	TTTGGCTTTTTGACCCCATA	
rps12_exon2R	CGTAAAGTTGCCAGAGTACGA	
rps12 intron1R	GGAGCCGTATGAGGTGAAAA	
rps12-int1a-2	GAATCGAGTTCGTCCATTCTATTT	
rps12 intron2R	TGTGGAAAGCCGTATTCGAT	
QC0130F	GCTCCTTCACGCAGTTCTTC	
atpF intronR	TTCGGGAAGGGATCATAGAA	
QCclpP exon2F	AATAAGTTGATTCGAGATTTCGGT	
clpP intron1R	GAACCGTATGCACCAAAAGG	
QC0670R	GTGATGGTTTCGCGAAGTTT	
clpP intron2R	TCATTCTGCGAAATAGAAAAACC	
ndhAF	TTGACGCCACAAATTCCAT	
ndhA intronR	AGGCCAAGACCTCATGTACG	

Table S2. A list of antibodies used in this study.

Antibody	Full Name of detected proteins	Host	Dilution	Source
AOX1a	Alternative oxidase 1A	Rabbit	1:1,000	Agrisera (AS04 054)
ATPC	Gamma subunit of ATP synthase	Rabbit	1:5,000	Agrisera (AS08 312)
ATPF	CF0I subunit of ATP synthase	Rabbit	1:5,000	Agrisera (AS10 1604)
ATPβ	Beta subunit of ATP synthase	Chicken	1:5,000	Agrisera (AS05 085)
CAL	Gamma-type carbonic anhydrase like	Mouse	1:5,000	(11)
Cox1	Cytochrome oxidase subunit I	Mouse	1:1,000	Abcam
Cox2	Cytochrome oxidase subunit II	Rabbit	1:1,000	Agrisera (AS04 053A)
CYT c	Cytochrome c	Rabbit	1:5,000	Agrisera (AS08 343A)
HA (clone 3F10)	Human influenza hemagglutinin protein epitope	Rat	1:500	Roche (11867423001)
Nad9	NADH-ubiquinone oxidoreductase chain 9	Rabbit	1:5,000	(12)
nMAT2	nuclear-encoded maturase 2	Rabbit	1:200	(10)
PetA	Photosynthetic electron transfer A	Rabbit	1:2,000	Agrisera (AS08 306)
PetB	Photosynthetic electron transfer B	Rabbit	1:5,000	Agrisera (AS18 4169)
PC	Plastocyanin	Rabbit	1:2,000	Agrisera (AS06 141)
Porin	The channel‐forming protein	Mouse	1:500	(13)
PsaD	Photosystem I subunit D	Rabbit	1:1,000	Agrisera (AS09 461)
PsbD	Photosystem II reaction center protein D	Rabbit	1:5,000	Agrisera (AS06 146)
RISP	Rieske iron-sulfur protein	Rabbit	1:5,000	(14)
Rpl16	Ribosomal protein L16 (mitochondrial)	Rabbit	1:1000	Agrisera (AS15 3069)
Rpl2	Ribosomal protein L2 (chloroplastic)	Rabbit	1:3,000	Agrisera (AS15 2876)
Rps1	Ribosomal protein S1 (chloroplastic)	Rabbit	1:1,000	Agrisera (AS15 2875)
Rps12	Ribosomal protein S12 (chloroplastic)	Rabbit	1:10,000	Agrisera (AS12 2114)
RPS14	Ribosomal protein S14 (mitochondrial)	Rabbit	1:1000	Agrisera (AS16 4094)
Rps7	Ribosomal protein S7 (chloroplastic)	Rabbit	1:3000	Agrisera (AS15 2877)
Tubulin	α-subunit of tubulin	Mouse	1:5,000	Sigma (T5168)
ZM-mTERF4	Maize mTERF protein 4	Rabbit	1:3,000	(15)

Table S3. Accession numbers of proteins used in phylogenetic analyses.

Speices	Accession numbers	Taxon
Arabidopsis thaliana	AT3G22450	Dicotyledons
	AT5G27820	
	AT1G08845	
	AT2G43310	
	AT3G45020	
	AT1G48350	
	AT3G20230	
	AT1G14205	
	AT3G25520	
	AT5G39740	
Brassica napus	CDY15088.1	
	CDY15089.1	
	CDY27889.1	
	CDY50258.1	
	CDY52293.1	
	CDY52294.1	
	XP013655608.1	
	XP013688027.1	
	XP013712154.1	
	XP013716293.1	
	XP013721243.1	
	XP013725072.1	
	XP013751606.2	
	XP022547979.1	
Capsella rubella	XP006282684.1	
	XP006284123.1	
	XP006286599.2	
	XP006292041.1	
	XP006296106.1	
	XP006296719.1	
	XP006298484.2	
	XP006299139.1	
	XP006304252.1	
	XP006305667.1	
	XP006306511.1	
Carica papaya	XP021889519.1	
	XP021890576.1	
	XP021893220.1	
	XP021896089.1	
	XP021900355.1	
	XP021907220.1	

	XP021912055.1	
	XP021912150.1	
Citrus clementina	XP006419937.1	
	XP006423824.1	
	XP006431833.1	
	XP006433150.1	
	XP006438704.1	
	XP006441940.1	
	XP006443043.2	
	XP024040181.1	
Populus trichocarpa	013G128600	
	014G174000	
	014G197100	
	019G099000	
	XP002319579.1	
	XP006376245.2	
	XP006384940.2	
	XP024444949.1	
	XP024460627.1	
	XP024461911.1	
	XP024463433.1	
	XP024465464.1	
Theobroma cacao	XP007014073.2	
	XP007016846.1	
	XP007030107.1	
	XP007033701.1	
	XP007033969.2	
	XP007045886.2	
	XP007046074.2	
	XP007049513.1	
	XP017976202.1	
Vitis vinifera	G01038188001	
	XP002263231.1	
	XP002265052.1	
	XP002266607.2	
	XP002270819.1	
	XP002276553.1	
	XP002276584.3	
	XP002278526.1	
	XP002283176.1	
Brachypodium distachyon	Bradi1g13630	Monocotyledons
	Bradi4g13640	
	Bradi5g09500	
	XP003562022.1	

	XP003563357.1	
	XP003566477.2	
	XP003570130.1	
	XP003574328.1	
	XP010238469.1	
	XP014757091.1	
Sorghum bicolor	001G517600	
	003G387900	
	XP002446092.1	
	XP002462788.1	
	XP002463594.1	
	XP002465793.1	
	XP002467495.1	
	XP021313879.1	
	XP021319899.1	
Oryza sativa Japonica	Os01g0896700	
	Os01g0896800	
	XP015610976.1	
	XP015614406.1	
	XP015614437.1	
	XP015623581.1	
	XP015625168.1	
	XP015630413.1	
	XP015630739.1	
Zea mays	NP001150322.1	
	NP001151288.1	
	NP001361504.1	
	NP001361506.1	
	XP008646075.1	
	XP008651469.1	
	XP008653044.1	
	Zm00001d012161	
	Zm00001d027512	
	Zm00001d042525	
Picea sitchensis	ABK22610.1	Gymnosperms
	ABK23983.1	
	ABK25907.1	
	ABK27001.1	
	ABR17003.1	
Selaginella moellendorffii	XP002963369.2	Bryophytes
	XP002966231.2	
	XP002971921.2	
	XP002974657.2	
	XP002974855.2	

	XP002989809.2	
	XP002993055.2	
	XP024521899.1	
Physcomitrella patens	PP00038G01610	
	PP00097G00560	
	PP00364G00030	
	PP00371G00150	
	XP024368324.1	
	XP024369260.1	
	XP024375627.1	
	XP024376468.1	
	XP024379707.1	
	XP024388120.1	
	XP024394632.1	
Marchantia polymorpha	PTQ36989.1	
	PTQ42040.1	
Ostreococcus lucimarinus CCE9901	XP001418789.1	Chlorophyta
Ostreococcus tauri	XP022839521.1	
Chlamydomonas reinhardtii	XP001690256.1	
Volvox carteri f.nagariensis	XP002948447.1	
Klebsormidium nitens	GAQ88143.1	Bacteria
Synechocystis sp.	AGF51023.1	
Nostoc punctiforme	RCJ34281.1	
Oscillatoria acuminata	WP015148985.1	
Rickettsia akari	WP012149889.1	
Escherichia coli	WP076797619.1	
Drosophila melanogaster	NP_610818.1	Animalia
Homo sapiens	NP_054880.2	
Mus musculus	NP_080586.1	
Heimdallarchaeota archaeon	OLS23692.1	Archaeal
Odinarchaeota archaeon	OLS18045.1	
Vulcanisaeta distributa	WP_013337397.1	
Zestosphaera tikiterensis	PUA33404.1	

Table S4. Pigment content and chlorophyll fluorescence parameters in wild-type and *ul18-l8* mutant plants.

Parameter	Col-0		*ul18-l8-1*		*ul18-l8-2*	
Water content (% fresh weight)	90.94 ± 0.29	**a**	92.52 ± 1.55	**a**	92.37 ± 0.37	**a**
Total chlorophyll (µg/mg fresh weight)	0.632 ± 0.081	**a**	0.540 ± 0.077	**a**	0.541 ± 0.096	**a**
Carotenoids (µg/mg fresh weight)	0.086 ± 0.015	**a**	0.075 ± 0.009	**a**	0.076 ± 0.012	**a**
Chlorophyll a/b	2.37 ± 0.07	**a**	2.28 ± 0.05	**a**	2.248 ± 0.22	**a**
Fv/Fm	0.837 ± 0.012	**a**	0.743 ± 0.064	**b**	0.739 ± 0.022	**b**
qL	0.755 ± 0.073	**a**	0.451 ± 0.777	**b**	0.476 ± 0.009	**b**
NPQ max	2.127 ± 0.287	**a**	2.622 ± 0.257	**b**	2.589 ± 0.186	**b**
NPQ relax	0.666 ± 0.130	**a**	0.690 ± 0.211	**a**	0.673 ± 0.108	**a**

Data are presented as means ± SD (n=4). Grouping information using the Fisher Method and 95% confidence is given by bold lowercase letters.

SI References

1. J. M. Alonso *et al.*, Genome-wide insertional mutagenesis of *Arabidopsis thaliana*. *Science* **301**, 653 (2003).
2. T. Nakagawa *et al.*, Development of series of gateway binary vectors, pGWBs, for realizing efficient construction of fusion genes for plant transformation. *J Biosci Bioeng* **104**, 34-41 (2007).
3. M. Uyttewaal *et al.*, Characterization of Raphanus sativus pentatricopeptide repeat proteins encoded by the fertility restorer locus for Ogura cytoplasmic male sterility. *Plant cell* **20**, 3331-3345 (2008).
4. J. J. McDermott, K. P. Watkins, R. Williams-Carrier, A. Barkan, Ribonucleoprotein capture by in vivo expression of a designer pentatricopeptide repeat protein in Arabidopsis. *Plant Cell* **31**, 1723–1733 (2019).
5. C. Wang, F. Aubé, M. Quadrado, C. Dargel-Graffin, H. Mireau, Three new pentatricopeptide repeat proteins facilitate the splicing of mitochondrial transcripts and complex I biogenesis in Arabidopsis. *J Exp Bot.* **69**, 5131-5140 (2018).
6. N. Haili *et al.*, The MTL1 Pentatricopeptide Repeat Protein Is Required for Both Translation and Splicing of the Mitochondrial NADH DEHYDROGENASE SUBUNIT7 mRNA in Arabidopsis. *Plant Physiol.* **170**, 354-366 (2016).
7. A. F. de Longevialle *et al.*, The pentatricopeptide repeat gene OTP51 with two LAGLIDADG motifs is required for the cis-splicing of plastid ycf3 intron 2 in Arabidopsis thaliana. *Plant J.* **56**, 157-168 (2008).
8. J. Van Leene *et al.*, Isolation of transcription factor complexes from Arabidopsis cell suspension cultures by tandem affinity purification. *Methods Mol. Biol.* **754**, 195-218 (2011).
9. A. R. Wellburn, The spectral determination of chlorophylls a and b, as well as total carotenoids, using various solvents with spectrophotometers of different resolution. *J. Plant Physiol.* **144**, 307-313 (1994).

10. I. Keren *et al.*, AtnMat2, a nuclear-encoded maturase required for splicing of group-II introns in Arabidopsis mitochondria. *RNA* **15**, 2299-2311 (2009).

11. S. Sunderhaus *et al.*, Carbonic anhydrase subunits form a matrix-exposed domain attached to the membrane arm of mitochondrial complex I in plants. *J. Biol. Chem.* **281**, 6482-6488 (2006).

12. L. LAMATTINA, D. GONZALEZ, J. GUALBERTO, J. M. GRIENENBERGER, Higher plant mitochondria encode an homologue of the nuclear ‐ encoded 30 ‐ kDa subunit of bovine mitochondrial complex I. *FEBS J.* **217**, 831-838 (1993).

13. N. L. Taylor *et al.*, Environmental stresses inhibit and stimulate different protein import pathways in plant mitochondria. *FEBS Lett.* **547**, 125-130 (2003).

14. C. Carrie *et al.*, Conserved and novel functions for Arabidopsis thaliana MIA40 in assembly of proteins in mitochondria and peroxisomes. *J. Biol. Chem.* **285**, 36138-36148 (2010).

15. K. Hammani, A. Barkan, An mTERF domain protein functions in group II intron splicing in maize chloroplasts. *Nucleic Acids Res.* **42**, 5033-5042 (2014).